科学出版社 出版
中国地理学会环境遥感分会
中国科学院遥感与数字地球研究所 主办

JOURNAL OF REMOTE SENSING
遥感学报

2013年 Vol.17 第17卷 No.4 第4期 ISSN 1007-4619 CN11-3841 / TP CODEN YXAUAB

2010年中国土地覆被遥感监测数据集（ChinaCover2010）

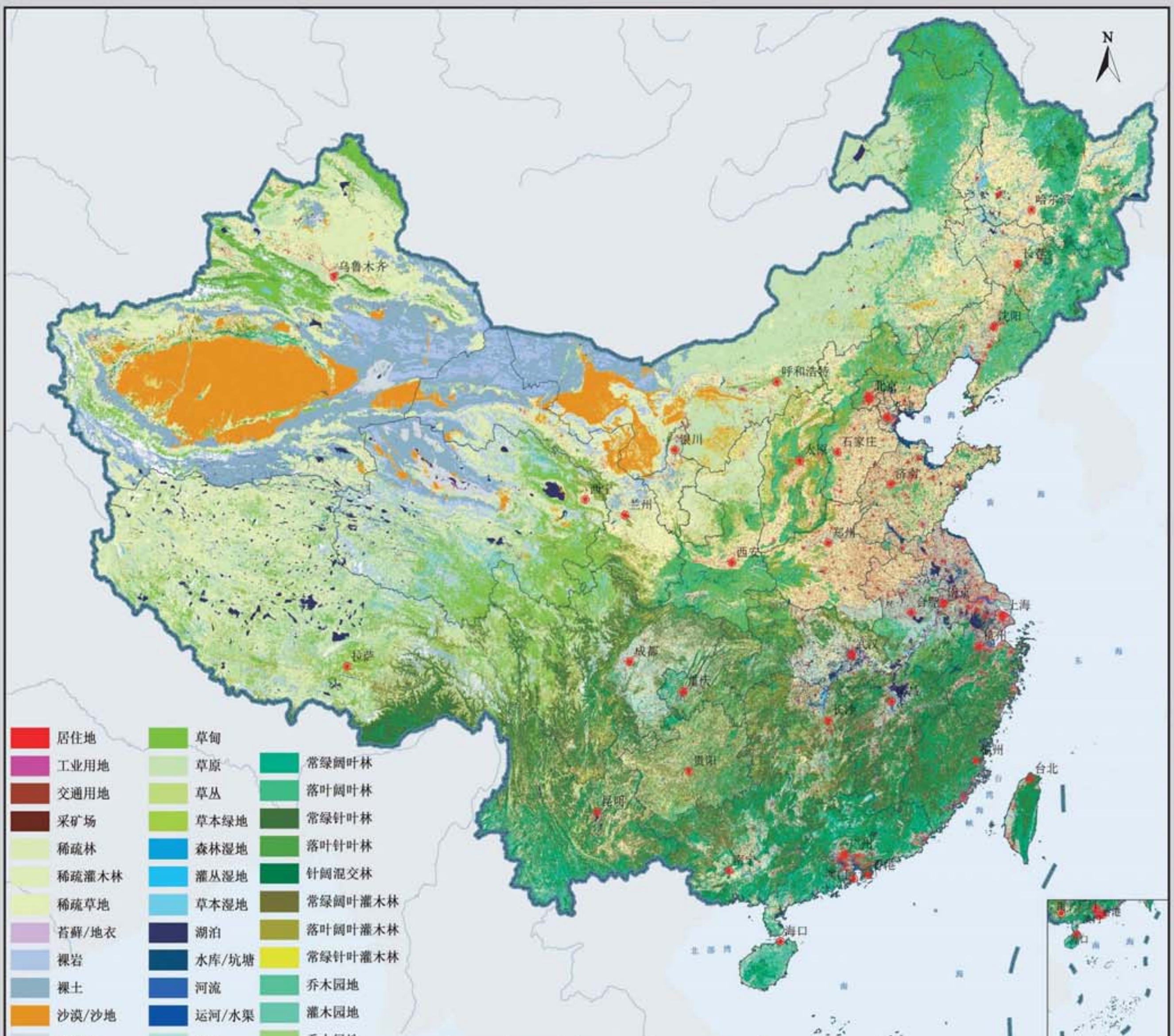

百种中国杰出学术期刊

遥感学报

Yaogan Xuebao

第 17 卷　第 4 期　2013 年 7 月

目　次

JOURNAL OF REMOTE SENSING

(**Vol. 17 No. 4 July, 2013**)

CONTENTS

(to be continued to Inside Back Cover)

(continued from Contents page)

Haze: Remote Sensing

Observation of atmospheric boundary layer height by ground-based LiDAR during haze days

ZHANG Wanchun[1,2], ZHANG Ying[1,2], LV Yang[1,2], LI Kaitao[1,2], LI Zhengqiang[1]

1. *State Environmental Protection Key Laboratory of Satellite Remote Sensing, Institute of Remote Sensing and Digital Earth of Chinese Academy of Sciences, Beijing* 100101, *China*;
2. *University of Chinese Academy of Sciences, Beijing*, 100049, *China*

Abstract: In order to investigate characteristics of atmospheric boundary layer height (ABLH) during haze pollution, we used ground-based CE370-C micro pulse LiDAR to derive the ABLH during January 2013 over Beijing, based on the gradient method. We find that the ABLH in severe haze days is lower than that in weak haze days and beneath about 500 m, with daily averaged value of about 424 m. The ABLH has negative correlation with the concentration of surface $PM_{2.5}$. The comparison of LiDAR observation with radiosonde detection is also presented in the paper and results show that two approaches have good consistency with difference less than about 86 meters.

Key words: haze, atmospheric boundary layer height, LiDAR, gradient method

CLC number: TP79 **Document code**: A

Citation format: **Zhang W C, Zhang Y, Lv Y, Li K T and Li Z Q. 2013. Observation of atmospheric boundary layer height by ground-based LiDAR during haze days. Journal of Remote Sensing, 17(4): 981–992 [DOI: 10.11834/jrs.20133075]**

1 INTRODUCTION

With the rapid economic expansion and the development of urbanization, haze pollution has become increasingly serious. In recent years, haze weather has aroused people's widely concerns in China. Haze whether is also an important indicator of the air quality (Wu, et al., 2007; Wu, 2006). Therefore the research on characteristics of haze is a hotspot in the field of atmospheric pollution (Gu, et al., 2010; Huang, et al., 2012).

The atmospheric boundary layer is the main district in which haze weather occurred. The atmospheric boundary layer, which usually refers to the area directly influenced by the ground in the troposphere, has the closest relationship with human activities and ecological environment. It responses to surface effect in a time scale of 1 hour or less (Hu, et al., 2003).Moreover, the atmospheric boundary layer height is one of important parameters in the research of remote monitoring particulate matters near the ground (Zhang & Li, 2013). Active LiDAR detection technique is an effective approach for observing the atmospheric boundary layer height (He & Mao, 2004; Yang, et al., 2005; Liu, et al., 2006; Pan, et al., 2010; Tsaknakis, et al., 2011; Wang, et al., 2012; Wu, et al., 2013; Griffiths, et al., 2013; Han, et al., 2007; Zhang, et al. 2004). In China, Qiu, et al. (2003) carried out detection experiment of high cloud and aerosol in the troposphere based on the multi-wavelength LiDAR. Mao, et al. (2006, 2007) determined the vertical distribution and changes of urban boundary layer height using LiDAR, and gave a preliminary analysis of the ground meteorological environment impacts on the diurnal variation of the boundary layer. Wang, et al. (2008) studied atmospheric boundary layer structure characteristics during summer in Beijing, as well as the extinction characteristics of atmospheric aerosols in the atmosphere boundary layer.

However, there are few studies on the atmospheric boundary layer height during severe haze weather detected by ground-based LiDAR. In order to investigate the characteristics of the haze whether in Beijing during January of 2013, in this paper, we determine the ABLH and the changes of atmospheric boundary layer under the haze weather, using ground-based micro-pulse LiDAR, as well as validating the result with the ABLH derived from the radiosonde observation. We also discuss the boundary layer height changes during the haze event, and study the relationship of its changes versus particle concentration of surface $PM_{2.5}$.

2 INSTRUMENT AND METHODS

2.1 Observation instrument and data

LiDAR used in this study is located at Institute of Remote Sensing and Digital Earth (RADI), Chinese Academy of Sciences (CAS), (40.00° N, 116.38° E), named CE370-C micro-pulse

Received: 2013-04-07; **Accepted**: 2013-05-24; **Version of record first published**: 2013-05-31

Foundation: "Strategic Priority Research Program-Climate Change: Carbon Budget and Relevant Issues" of the Chinese Academy of Sciences (No. XDA05100202); National Major Scientific Research Program (No.2010CB950800, 2010CB950801)

First author biography: ZHANG Wanchun (1986—), female, Ph.D. candidate, she majors in atmospheric aerosol remote sensing. E-mail: wanchun950@163.com

Corresponding author biography: LV Yang (1984—), female, research assistant, she majors in atmospheric aerosol remote sensing. E-mail: lvyang@irsa.ac.cn

LiDAR and produced by CIMEL company in France. The diameter of laser transmitter system is 20 cm, which is used to expand laser beam through a refracting telescope. The receiver system includes two parts: standard module and low altitude module. The measurement of standard module ranges from 0.3 km to 30 km, while the low altitude module from 0.1 km to 3 km. Both vertical spatial resolutions are 15 m. In this paper, we use the signal received from standard module. After the residual impulse, background, range and overlap corrections, we can derive the range corrected signal (RCS). Using the signal changes and cooperating with aerosol backscatter extinction profile information, we can estimate the height of the atmospheric boundary layer.

The radiosonde data, which used for comparison with LiDAR in the study, is measured at Southern Observatory (site 54511) in Beijing (39.80° N, 116.47° E), including pressure, height, temperature, humidity, vapor mixing ratio, potential temperature, wind speed and wind direction. Moreover, we reprocess vapor mixing ratio and potential temperature information to estimate the ABLH based on radiosounde method presented by Liu (1990).

2.2 Atmospheric boundary layer height observation by LiDAR

2.2.1 *Gradient method*

Gradient method is commonly used to detect the ABLH by LiDAR. LiDAR signal intensity corresponds to the concentration of atmospheric aerosol particles. Due to the effect of warm cover of the inversion layer, most of atmospheric aerosol particles concentrate in atmospheric boundary layer. Therefore, between atmosphere boundary layer and free atmosphere, the concentration of atmospheric aerosol particles will change sharply (Lammert & Bosenderg, 2005; Hennemuthet & Lammert, 2006; Wang, et al., 2008; Pan, et al., 2010). Therefore, RCS gradient profile represents the atmospheric aerosol vertical distribution gradient changes. LiDAR backscatter signal can be expressed in Eq.(1) (Klett, 1981; Fernald, et al., 1972)

$$P(r) = P_0 \frac{c\tau}{r^2} A \frac{\beta(r)}{r^2} \exp\left[-2\int_0^r \sigma(r')\mathrm{d}r'\right] \tag{1}$$

where $P(r)$ is the backscatter intensity received from the distance r, P_0 is the intensity emitted by the laser; c is a constant of laser radar system, τ is duration of impulse of the laser, A is the geometric correction factor, $\beta(r)$ and $\sigma(r)$ are backscatter extinction and total extinction coefficients, respectively.

A derivative of the range corrected signal ($\mathrm{RCS}=P(r)r^2$) can be represented as:

$$\mathrm{DEV}(r) = \mathrm{d}(\mathrm{RCS})/\mathrm{d}r \tag{2}$$

where DEV is the derivation of RCS with respect to r. The vertical position corresponding to the minimum value of DEV is therefore the height of the atmospheric boundary layer, where the concentration of aerosol particles within the atmosphere changes fastest.

2.2.2 *Radiosonde method*

Radiosonde method (Liu, 1990) can be used to determine the ABLH based on radiosonde data, which comprise wind direction (D), wind speed (V), mixing ratio (S), potential temperature (θ) and temperature (t), within and beyond the boundary layer. Within the boundary layer, due to the fully turbulent mixing effects, various physical properties of the atmosphere in the vertical direction tend to be uniform (Liu, 1990; Liao, 2005). In the boundary layer it should be satisfied with the following criterions

(1) $\frac{\partial\theta}{\partial z} = 0, \frac{\partial S}{\partial z} = 0$

(2) $r > r_d$ 或 $r = r_d$

(3) D and V are consistent (except for the range from the ground to 10 or dozens of meters).

where, r is the atmospheric temperature lapse rate and r_d is the dry adiabatic lapse rate.

Based above method, using radiosonde data, we can determine the atmospheric boundary height. However, as a result of using tethered sounding, this method is constrained by the length of tether line, which is usually less than about 1000 m. Therefore this method is somewhat limited in the application (Liu, 1990; Liao, 2005).

3 OBSERVATION AND DATA PROCESSING

In this paper, we use micro-pulse LiDAR CE370-C to get the ABLH information during haze pollution of January 2013 in Beijing based on gradient method. In order to discuss the polluted level of the haze whether, we classify haze weather according to the Air Quality Index (AQI). The Air Quality Index greater than 100 corresponds to weak haze day, and more than 200 to severe haze day. Therefore, January 25, 2013 belongs to weak haze days with AQI of 104, and January 28 belongs to severe haze days with AQI of 398, those will be analyzed below.

Time resolution of this LiDAR is about 1 min. In this paper, in order to compare with radiosonde method, we use the hourly average LiDAR RCS. The vertical range of LiDAR observations is between 300 m and 1500 m. In the paper, we use the gradient method (flow diagram in Fig.1) to determine the ABLH.

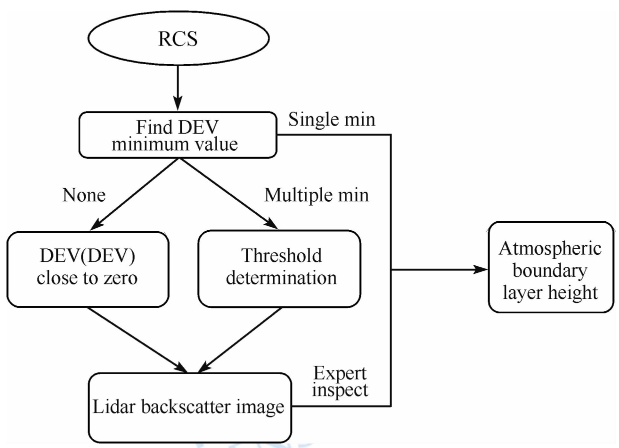

Fig.1 Flow chart of gradient method to detect the ABLH

Operation steps are:

(1) Calculate the derivative, DEV. If there is only one minimum value, the ABLH could be determined. As shown in Fig.2(a)(b), the minimum point of 420 m is the ABLH at 7:00 am on January 28.

(2) From 300 m to 1500 m, if there are multiple minimum values, the value between -10^9 and -10^7 is then used to get the extreme value point, with inspecting the continuous changes of the atmospheric profile signals and LiDAR backscatter image. As shown in Fig.2(c)(d), the possible ABLH is 645 m and 780 m. With LiDAR backscatter image, we can easily determine that 780 m is the ABLH at 4:00 am on January 26.

(3) From 300 m to 1500 m, if there is no minimum value, we need to calculate the derivative of DEV, noted by DEV(DEV). With the continuous changes of the atmospheric boundary layer and LiDAR backscatter image, we need to perform expert judgments. According to our experience, the minimum value after the first jump is the ABLH. As shown in Fig.2(e)(f)(g), down from 1500 m, the DEV(DEV) curve after the first jump tends to be zero at 450 m, which is the ABLH at 8:00 am on January 28. Moreover, LiDAR backscatter image confirms this.

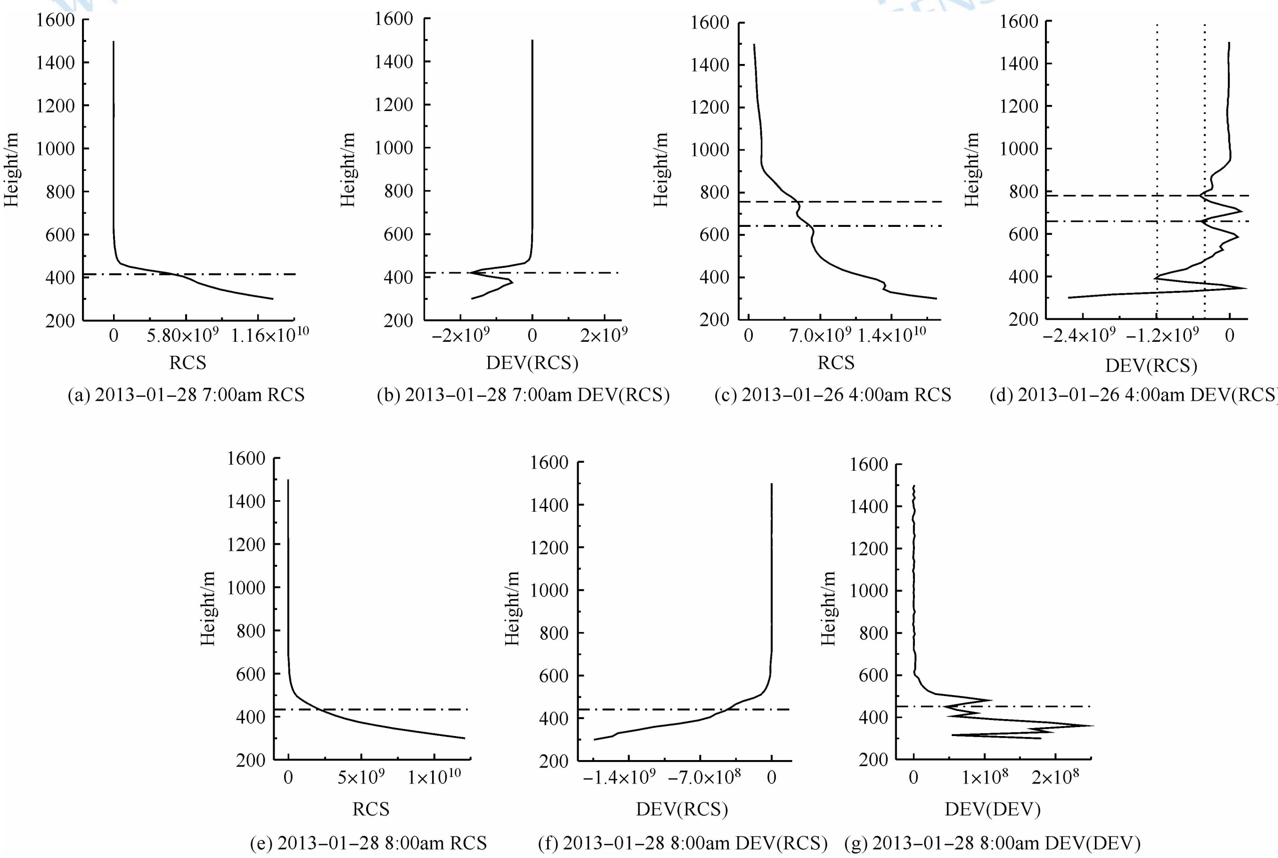

Fig.2 Interpretation of the gradient method to detect the ABLH

(for (a)(b), the dot lines represent the minimum value position; for(c)(d), the horizontal dot lines indicate the location of minimum value positions under the threshold range, while the perpendicular dot lines represent the threshold range; for (e)(f)(g), the dot lines represent that DEV (DEV) tend to zero after the first jump from top to bottom)

Fig.3(a) shows the daily variation of the ABLH on January 25 and January 28. Lines in this figure represent the hourly average ABLH from LiDAR. It can be seen that the boundary layer height is up to 1100 m on January 25 (weak haze day), and at night the value is roughly between 700 m and 1000 m. The boundary layer height has no obvious changes between day and night, continuously between 300 m and 500 m on January 28 (severe haze day). Fig.3 (b) and Fig.3 (c) show comparison of water vapor mixing ratio and potential temperature on January 25 and January 28, respectively. It shows that water vapor mixing ratio on January 28 is obviously higher than that on January 25. Namely, on January 25, vertical changes of water vapor mixing ratio reflects the ABLH position. However, on January 28, potential temperature vertical changes have an obvious temperature inversion, which suggests that in the severe haze days, the boundary layer is stable. Therefore, with the increase of the degree of haze pollution, day time and night time changes of the ABLH decrease significantly. Especially, during severe haze weather, the ABLH diurnal variation is not obvious, and the ABLH is averagely about 500 m lower than that of weak haze days.

We analyze the characteristics of an increasing haze process from January 25 to January 28. Fig.3 shows the comparisons of ABLH with PM2.5 concentration and average wind speed from January 25 to January 28, respectively. All data are shown as daily average. In Fig.4(a), with gradually increase of the haze, the boundary layer height decreases and $PM_{2.5}$ concentration increases. The main reason for this phenomenon can be explained by the wind speed, which is almost constant between 1.35 m/s and 1.61 m/s as shown in Fig.4(b). No wind or breeze makes atmospheric turbulence weaken, and ABLH becomes steady. The pollutant concentration increases quickly, and then the serious pollution is formed.

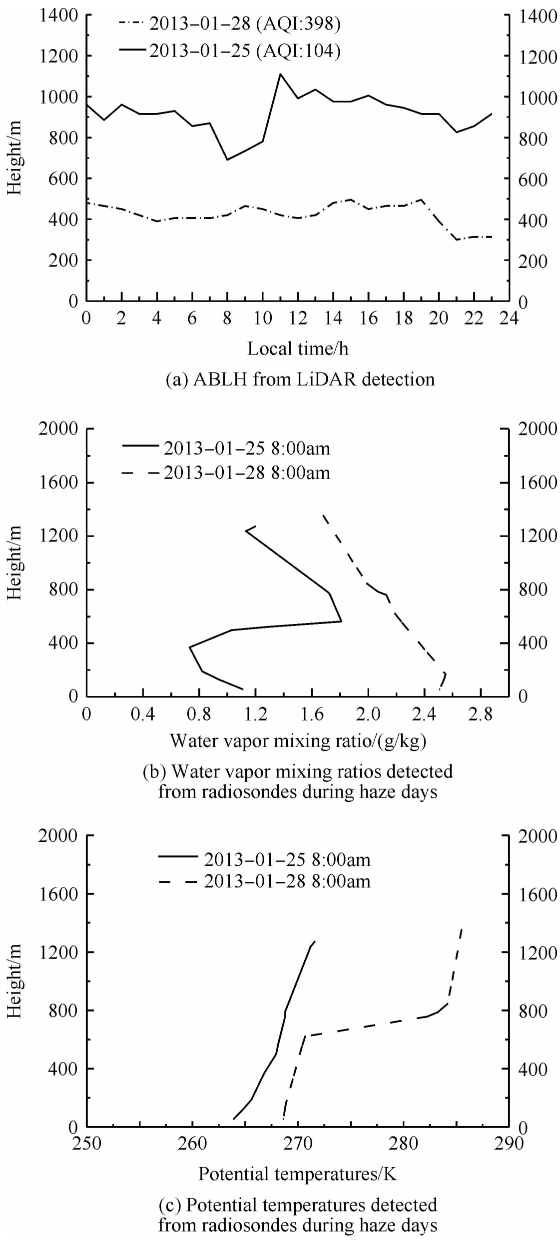

Fig.3 (January 25 and 28, 2013, Beijing) ABLH from LiDAR detection, water vapor mixing ratios detected from radiosondes, and potential temperatures detected from radiosondes

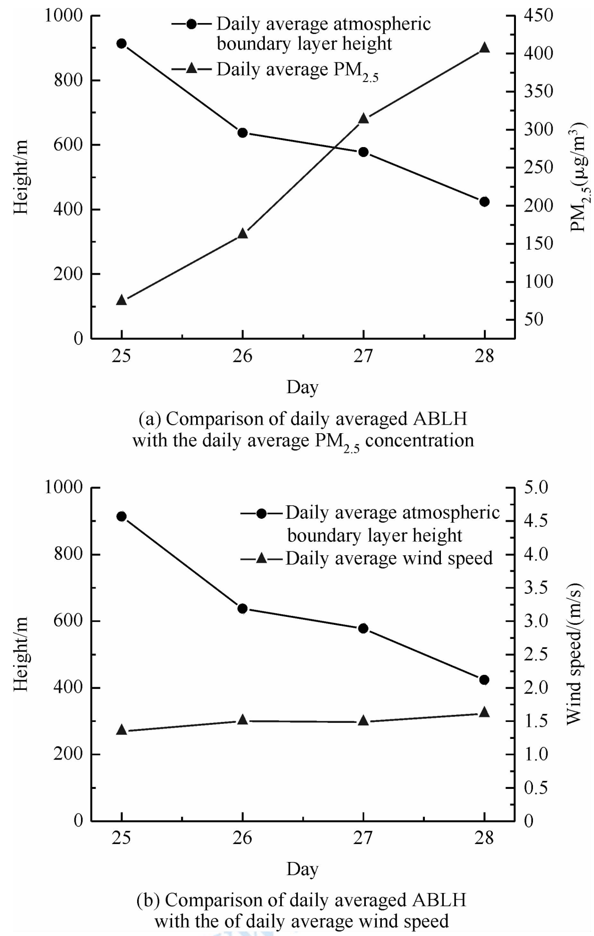

Fig.4 Relations among ABLH, PM2.5 and wind during haze days on January 25 and 28, 2013

4 COMPARISON AND ANALYSIS

In order to validate LiDAR observation, we derive the ABLH by radiosonde approach based on the atmospheric sounding data in January of 2013, with two values at 8:00 am and 20:00 pm each day. The relative error of this method compared with the dry adiabatic curve method is between 2.7% and 15% (Liu, 1990). In this article, we perform a comparative analysis on the ABLH obtained from LiDAR and radiosonde during haze whether with the AQI higher than 100. Fig. 5 is the ABLH histogram from these two methods. It can be seen that the monthly average ABLH detected from LiDAR is about 575 m, and the standard deviation is 155 m. Meanwhile, the ABLH of radiosonde is about 590 m and the standard deviation is 178 m. It shows that the ABLHs detected from two methods agree well, with the monthly average difference of ABLH about 86 m. Considering the spatial distance between these two stations, the difference between these two methods is acceptable.

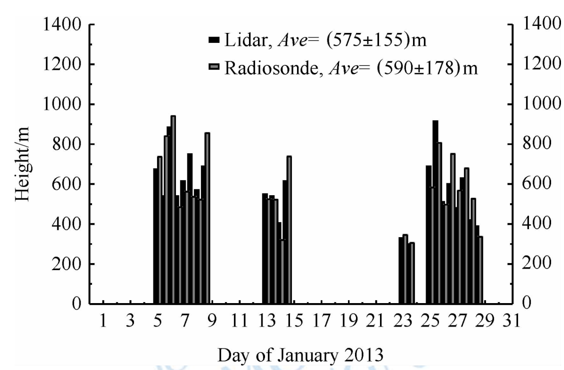

Fig.5 Histogram of the ABLH obtained from LiDAR and radiosonde in January of 2013 at Beijing

Advantage of LiDAR observation is its continuous real-time detecting capability. Real-time monitoring of boundary layer height can be used in the haze monitoring, and the gradient method is an effective method in this detection. However, gradient method used to detected ABLH has shortcomings in two aspects: Firstly, when weather is clear, the atmospheric aerosol extinction is weak and it is difficult to find RCS derivative profile change position. Then, when there are lots of clouds led to multiple minimum points of signal derivative, it will need expert interpretation to determine cloud height, and distinguish clouds from aerosols.

5 CONCLUSIONS

We derived the ABLH from LiDAR measurements based on gradient method in January 2013 in Beijing. We analyzed the relationship between ABLH and related parameters, such as $PM_{2.5}$ concentration, average wind speed, and get the following conclusions:

(1) On the detection ability, the traditional meteorological observation approach, e.g., radiosonde method due to the limited frequency of detectionis difficult to obtain continuous information. However, the gradient method based on LiDAR is an effective method to obtain continuous ABLH during haze days.

(2) During haze days, ABLH has obvious a downward trend. In severe haze days, the averaged ABLH is about 300—500 m. By comparison with weak haze days, the ABLH of severe haze days can continues a long time to lower, e.g., during a day and night, which aggravates the accumulation of atmospheric pollutants.

(3) By comparing ABLH obtained from LiDAR with the surface $PM_{2.5}$ concentration on January 25 and January 28 during the haze pollution, we find that ABLH and $PM_{2.5}$ concentration are significantly negatively correlated, the lower the atmospheric boundary layer, the higher $PM_{2.5}$ concentration.

The ABLH is of great interests to the remote sensing of particulate matter mass concentration near ground. Our LiDAR results show good consistency with radiosonde detection during sever haze, which can be used in the relevant researches on the aerosol vertical distribution.

Acknowledgements: We thank to the public weather service center of China meteorological administration to provide the radiosonde data.

REFERENCES

Fernald F G, Herman B M and Reagan J A. 1972. Determination of aerosol height distributions by lidar. Journal of Applied Meteorology, 11 (3): 482 − 489 [DOI: 10.1175/1520 − 0450 (1972) 011 < 0482: DOAHDB>2.0.CO;2]

Griffiths A D, Parkes S D, Chambers S D, Mccabe M F and Williams A G. 2013. Improved mixing height monitoring through a combination of lidar and radon measurements. Atmospheric Measurement Techniques, 6(2):207−218 [DOI: 10.5194/amt−6−207−2013]

Han D W, Liu W Q, Zhang Y J, Liu J G., Lu Y H., Zhao N J., Yang H., Yu T. 2007. Boundary layer aerosol monitoring by Lidar at Beijing in winter. Journal of Atmospheric and Environmental Optics, 2(2): 104−109

He Q S and Mao J T. 2004. Micro-pulse Lidar and its applications. Meteorological Science and Technology, 32(4):219−224

Hennemuth B and Lammert A. 2006. Determination of the atmospheric boundary layer height from Radiosonde and Lidar backscatter. Boundary-Layer Meteorology, 120 (1): 181 − 200 [DOI: 10.1007/s10546−005−9035−3]

Hu F, Hong Z X and Lei X E. 2003. Recent Progress of Atmospheric Boundary Layer Physics and Atmospheric Environment Research in IAP. Chinese Journal of Atmospheric Sciences, 27(4):712−728

Huang K, Zhuang G, Lin Y, Fu J S, Wang Q, Liu T, Zhang R, Jiang Y, Deng C, Fu Q, Hsu N C and Cao B. 2012. Typical types and formation mechanisms of haze in an Eastern Asia megacity, Shanghai. Atmospheric Chemistry and Physics, 12(1):105−124 [DOI:10.5194/acp−12−105−2012]

Klett J D. 1981. Stable analytical inversion solution for processing lidar returns. Applied Optics, 20(2):211−220 [DOI: 10.1364/AO.20.000211]

Lammert A and Bösenberg J. 2005. Determination of the convective boundary-layer height with laser remote sensing. Boundary-Layer Meteorology, 119(1):159−170 [DOI: 10.1007/s10546−005−9020−x]

Liao G L. 2005. Calculation Methods and Influence Factors of the Thickness of Atmospheric Mixed Layer. Journal of the Graduates Sun YAT-SEN University (Natural Sciences, Medicine), 26 (4):66−73

Liu C, Ming H, Wang P, Xie J P., Yang H., Zhao N J., Xie P H., Takeuchi N., Koike T. 2006. Measurements of the aerosol over Naqu of Tibet and suburb of Beijing by Micro-pulse Lidar(MPL). ACTA Photonica Sinic, 35(9):1435−1439

Liu Z P. 1990. Study on a method to ascertain mixing height. Research of Environmental Sciences, 3(1):8−12

Mao M J, Jiang W M, WU X Q, Qi F D., Yuan R M., Fang H T., Liu D., Zhou J. 2006. LIDAR exploring of the UBL in downtown. ACTA Science Circumstantiate, 26(10):1723−1728

Mao M J, Zhang Y C, Fang H T, Qi F D., Zhao S S., Hu H L., Zhou J. 2007. Detection of aerosol distribution by atmospheric environment airborne Lidar over Qingdao and adjacent sea area. Chinese Journal of Geophysics, 50(2):370−376

Pan G, Geng F H, Chen Y H, He Q S., Zhang H., Kang Y M., Mao X Q., Wang H Q. 2010. Analysis of a haze event by micro-pulse light laser detection and ranging measurements in Shanghai. ACTA Science Circumstantiate, 30(11):2164−2173

Qiu J H, Zhen S P, Huang Q R, Xia Q L, Yang L Q., Wang W M., Pan J D., Sun J H. 2003. Lidar measurements of cloud and aerosol in the upper troposphere in Beijing, Chinese Journal of Atmospheric Sciences, 27(1):1−7

Tsaknakis G, Papayannis A, Kokkalis P, Amiridis V, Kambezidis H D, Mamouri R E, Georgoussis G and Avdikos G. 2011. Inter-comparison of lidar and ceilometer retrievals for aerosol and planetary boundary layer profiling over Athens, Greece. Atmospheric Measurement Techniques, 4(6):1261−1273 [DOI: 10.5194/amt−4−1261−2011]

Wang Z, Cao X, Zhang L, Notholt J, Zhou B, Liu R and Zhang B. 2012. Lidar measurement of planetary boundary layer height and comparison with microwave profiling radiometer observation. Atmospheric Measurement Techniques, 5(8):1965−1972 [DOI: 10.5194/amt−5−1965−2012]

Wang Z Z, Li J, Zhong Z Q and Liu D. 2008. LIDAR exploration of atmospheric boundary layer over downtown of Beijing in summer. Journal of Applied Optics, 29(1):96−100

Wu D. 2006. More Discussions on the differences between haze and fog in city. Meteorological Monthly, 32(4):9−15

Wu D, Deng X J, Bi X Y, Li F., Tan H B. 2007. Distinguishing of fog or haze and the operational criteria for observation, forecasting and early warning of haze in urban areas of Guangdong, Hong Kong and Macau. Guangdong Meteorology, 29(2):5–28

Wu M, Wu D, Fan Q, Wang B M, Li H W and Fan S J. 2013. Study on the atmospheric boundary layer and its influence on regional air quality over the Pearl River delta. Atmospheric Chemistry and Physics Discussions, 13(3):6035–6066 [DOI:10.5194/acpd-13-6035-2013]

Yang H, Liu W Q, Lu Y H, Xie P H, Xu L., Zhao X S., Yu T., Yu J H. 2005. PBL observations by Lidar at Peking. Optical Technique, 31(2): 221–226

Zhang G X, Zhang Y C, Hu S X, Liu X Q, Shao S S, Yang G C, Deng M, Tan K, Hu H L. 2004. Measurements of planetary boundary layer aerosols with mobile Lidar AML-1. High Power Laser and Particle Beams, 16(3):286–290

Zhang Y and Li Z Q. 2013. Estimation of $PM_{2.5}$ from fine-mode aerosol optical depth. Journal of Remote Sensing, 17(4): 929–943 [DOI:10.11834/jrs.20133063]

利用激光雷达探测灰霾天气大气边界层高度

张婉春[1,2]，张莹[1,2]，吕阳[1,2]，李凯涛[1,2]，李正强[1]

1.中国科学院遥感与数字地球研究所 国家环境保护卫星遥感重点实验室，北京 100101；
2.中国科学院大学，北京 100049

摘　要：为了探测灰霾天气大气边界层高度变化的特征，利用 CE370-C 型微脉冲激光雷达观测了北京 2013 年 1 月严重灰霾期间的大气边界层高度。基于激光雷达距离校正回波信号，使用梯度法处理了严重灰霾天和轻度灰霾天的大气边界层观测数据，发现在灰霾天气时大气边界层高度显著降低，严重污染时的大气边界层高度低于 500 m，日平均高度约 424 m，且与 $PM_{2.5}$ 浓度呈现明显的负相关性。将激光雷达探测结果与探空数据进行了对比分析，结果显示激光雷达与探空数据观测结果有较好的一致性，两者在本次灰霾期间的平均差异约为 86 m。

关键词：灰霾，大气边界层高度，激光雷达，梯度法

中图分类号：TP79　　**文献标志码**：A

引用格式：张婉春，张莹，吕阳，李凯涛，李正强. 2013. 利用激光雷达探测灰霾天气大气边界层高度. 遥感学报，17(4)：981–992

Zhang W C, Zhang Y, Lv Y, Li K T and Li Z Q. 2013. Observation of atmospheric boundary layer height by ground-based LiDAR during haze days. Journal of Remote Sensing, 17(4): 981–992 [DOI: 10.11834/jrs.20133075]

1　引　言

由于经济规模的迅速扩大和城市化进程的加快，城市灰霾天气日趋严重。近年来，中国各地灰霾天气的频繁出现越来越引起人们的广泛关注。灰霾对空气质量有重要指示意义(吴兑，2006；吴兑 等，2007)，研究其分布特征是大气污染领域的一个热点(潘鹄 等，2010；Huang 等，2012)。

大气边界层是灰霾天气发生的主要区域。大气边界层通常是指受地面直接影响、并与地面有直接作用的对流层，与人类关系最为密切，是人类活动和各项生态环境过程发生和发展的主要气层。它响应地面作用的时间尺度为 1 小时或更短(胡非 等，2003)。大气边界层高度是遥感监测研究近地面颗粒物过程的重要参量(张莹和李正强，2013)。主动遥感的激光雷达探测技术(贺千山和毛节泰，2004；杨辉 等，2005；刘诚 等，2006；潘鹄 等，2010；Tsaknakis 等，2011；Wang 等，2012；Wu 等，2013；Griffiths 等，2013)，是探测大气边界层的有效手段(韩道文 等，2007；张改霞 等，2004)。邱金桓等人(2003)开展了基于多波长激光雷达的对流层高云和气溶胶探测实验；毛敏娟等人(2006，2007)利用激光雷达确定了城市边界层高度垂直分布及逐时变化，初步分析了地面气象环境对边界层日变化的影响；王珍珠等人(2008)研究了北京城区夏季大气边界层结构变化特征，以及大气边界层内大气气溶胶的消光特性。

然而，严重灰霾天气下的大气边界层高度等方面的研究还不多见，本文以 2013 年 1 月北京地区灰霾过程为例，针对灰霾天气下大气边界层变化，利用地基微脉冲激光雷达探测信号，确定大气边界层高度，并与探空数据对比分析，讨论了在灰霾期间的边界层高度变化，并与近地面颗粒物浓度的变化做了对比。

2　观测仪器与方法

2.1　观测仪器与数据

激光雷达位于中国科学院遥感与数字地球研

收稿日期：2013-04-07；**修订日期**：2013-05-24；**优先数字出版日期**：2013-05-31
基金项目：中国科学院战略性先到科技专项(编号：XDA05100202)；国家重大科学研究计划(编号：2010CB950800，2010CB950801)
第一作者简介：张婉春(1986—　)，女，博士研究生，现从事大气气溶胶遥感研究。E-mail: wanchun950@163.com
通信作者简介：吕阳(1984—　)，女，助理研究员，现从事大气气溶胶遥感研究。E-mail: lvyang@irsa.ac.cn

究所观测点(40.00° N, 116.38° E),雷达型号为CE370-C微型激光雷达,由法国CIMEL公司生产,激光雷达的激光发射器系统通过一个直径20 cm的折射望远镜扩展激光光束。接收器包括高空接收器和低空接收器两部分。高空接收器的有效测量范围为0.3—30 km;低空接收器的有效测量范围为0.1—3 km,垂直空间分辨率为15 m。本文使用高空接收器接收雷达原始回波信号,经过残留脉冲校正、背景校正、距离校正和重叠区校正,获得激光雷达距离平方校正回波信号RCS(Range Corrected Signal),利用该信号的变化,同时配合使用气溶胶后向散射消光廓线信息得到大气边界层的高度。

用于对比分析的数据为北京南郊气象观测站54511(39.80°N,116.47°E)探空资料,其中包括气压、大气层高度、温度、湿度、混合比(湿空气中的水汽质量与干空气质量之比)、位温、风速和风向等资料。利用探空法处理该资料中的混合比与位温信息,估计大气边界层高度(刘北平,1990)。

2.2 大气边界层高度探测方法

2.2.1 梯度法

激光雷达信号探测大气边界层垂直高度的常用方法是梯度法。激光雷达RCS信号廓线强度对应于相应高度大气气溶胶粒子浓度的大小。由于逆温的暖盖作用,大量的大气气溶胶富集在大气边界层内,因此大气边界层到自由大气层之间气溶胶的浓度就会发生变化(Lammert 和 Bösenberg,2005;Hennemuth 和 Lammert,2006;王珍珠 等,2008;潘鹄 等,2010)。RCS廓线梯度变化代表着大气气溶胶垂直分布梯度的变化。激光雷达接收的后向散射信号 $P(r)$ 的表达式(Klett,1981;Fernald 等,1972)为:

$$P(r) = P_0 \frac{c\tau}{r^2} A \frac{\beta(r)}{r^2} \exp\left[-2\int_0^r \sigma(r')\mathrm{d}r' \right] \quad (1)$$

激光雷达距离校正回波信号($\mathrm{RCS}=P(r)r^2$)的一阶导数可表示为:

$$\mathrm{DEV}(r) = \mathrm{d}[\mathrm{RCS}]/\mathrm{d}r \quad (2)$$

式中,$P(r)$是激光雷达接收到距离r处的后向散射回波信号,P_0是激光发射能量;c是激光雷达系统常数,τ是脉冲延时,A是几何校正因子,$\beta(r)$和$\sigma(r)$分别是目标后向散射消光系数和大气的总消光系数,DEV是激光雷达RCS信号对距离求导,DEV廓线最小值对应的垂直高度位置就是大气边界层的高度。在此高度上,大气气溶胶粒子浓度的梯度变化最快。

2.2.2 探空资料综合评定法

综合评定法(刘北平,1990)根据实测大气数据获取系统探空得到的风向D、风速V,混合比S、位温θ和温度t随高度的分布,以及上述气象要素在边界层内和边界层顶以上变化的差异,来确定大气边界层高度。在边界层内由于充分的湍流混合作用,大气的各种物理属性在垂直方向近似趋于均一(刘北平,1990;廖国莲,2005)。在边界层内应满足:

(1) $\dfrac{\partial \theta}{\partial z} = 0, \dfrac{\partial S}{\partial z} = 0$

(2) $r > r_\mathrm{d}$ 或 $r = r_\mathrm{d}$

(3)D,V基本保持一致(贴近地面十几米到几十米的气层内是例外的)。

式中,r表示大气温度递减率,r_d表示干绝热递减率。

综合评定法用实测探空资料直接确定大气边界厚度,但由于采用系留探空、高度受到系留线长度(常用的系留线长度约为1000 m)约束,该方法在应用上受到一定的限制(刘北平,1990;廖国莲,2005)。

3 数据处理和观测结果

利用微脉冲激光雷达CE370-C接收数据获取2013年1月大气边界层高度信息,对激光雷达在灰霾期间利用梯度法探测大气边界层高度的结果进行分析。按照空气质量指数AQI(Air Quality Index)对灰霾天气分级,空气质量指数大于100为轻度灰霾天气,大于200为严重灰霾天气。2013年1月25日AQI为104,属于轻度灰霾天气,1月28日AQI为398,属于严重灰霾天气,我们重点取这两天进行对比分析。

激光雷达观测RCS时间分辨率为1 min,本文均取激光雷达RCS信号的小时平均,为了便于与探空资料探测(常用的系留线长度约为1000 m)对比,取垂直高度为300—1500 m的RCS信号。

将梯度法原理应用到本文研究中,针对具体情况,流程图如图1所示:

具体操作如下:

(1)求RCS导数DEV,若有唯一极小值,则该高度为大气边界层高度,如图2(a)(b),420 m是唯一极小值点,即为2013-01-28 7:00 am大气边界层高度。

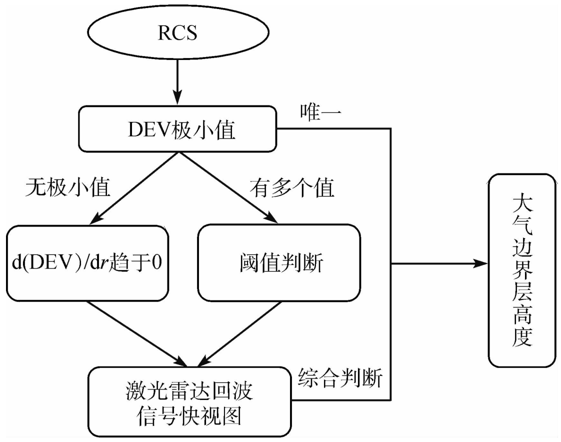

图 1　激光雷达探测大气边界层高度判读流程图

(2)在 300—1500 m 若有多个极小值，取阈值在 $(-10^9, -10^7)$之间的极值点，配合连续时间上大气边界层高度及激光雷达回波信号快视图颜色变化，确定大气边界层高度，如图 2(c)(d)符合阈值范围的是 645 m 和 780 m，配合激光雷达回波信号快视图确定 780 m 为 2013 年 1 月 26 日 4:00 am 大气边界层高度。

(3)在 300—1500 m 若无极小值，则求 DEV 的导数 DEV(DEV)，配合连续时间上大气边界层高度及激光雷达回波信号快视图颜色变化进行综合判断，根据经验，一般从 1500 m 向下第一个跳跃后的极小值即为大气边界层高度，如图 2(e)(f)(g)，从 1500 m 向下，曲线第一个跳跃后的 DEV(DEV)趋于 0 的位置为 450 m，配合激光雷达回波信号快视图确定 450 m 为 2013 年 1 月 28 日 8:00 am 大气边界层高度。

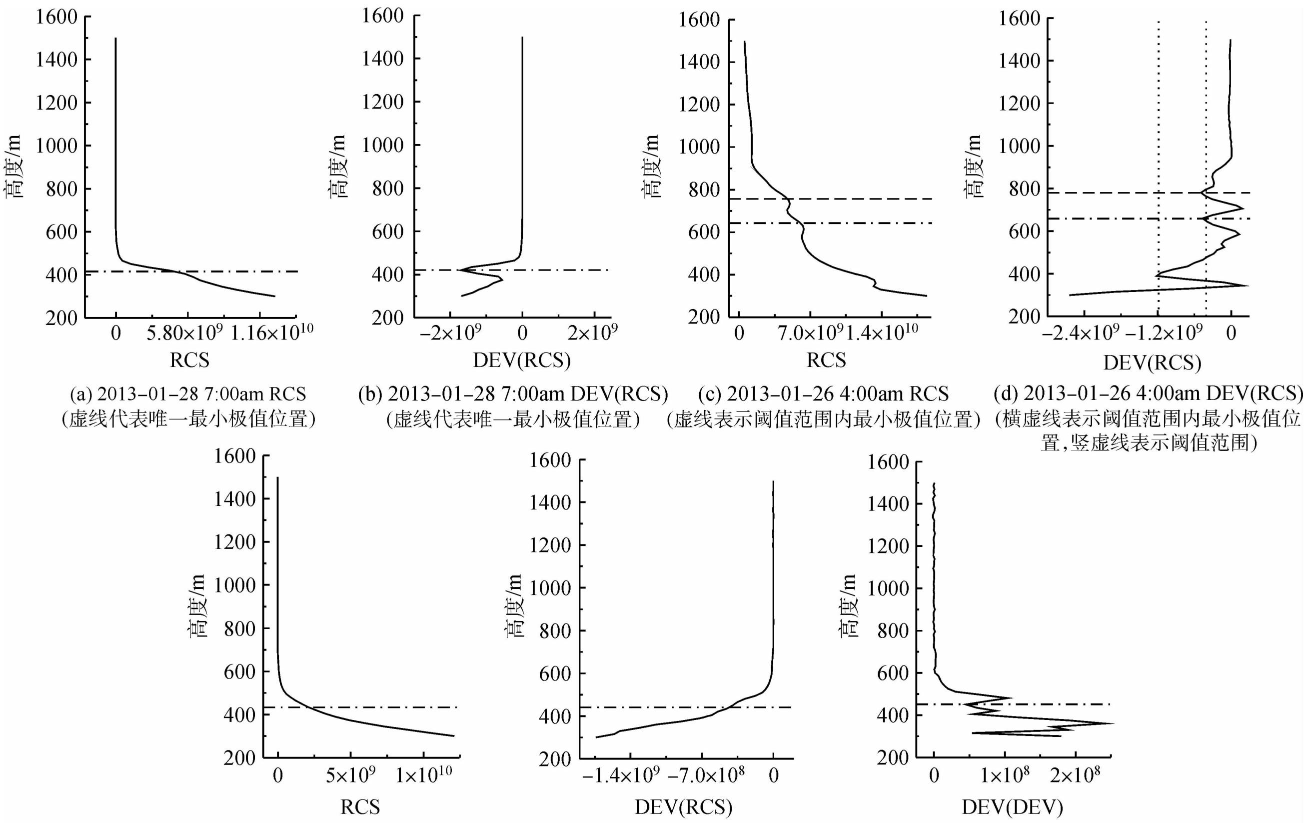

(a) 2013-01-28 7:00am RCS（虚线代表唯一最小极值位置）
(b) 2013-01-28 7:00am DEV(RCS)（虚线代表唯一最小极值位置）
(c) 2013-01-26 4:00am RCS（虚线表示阈值范围内最小极值位置）
(d) 2013-01-26 4:00am DEV(RCS)（横虚线表示阈值范围内最小极值位置，竖虚线表示阈值范围）
(e) 2013-01-28 8:00am RCS
(f) 2013-01-28 8:00am DEV(RCS)
(g) 2013-01-28 8:00am DEV(DEV)

图 2　激光雷达探测大气边界层高度判读结果
((e)—(g)中，虚线代表 DEV(DEV)从上往下第一个跳跃后的其值趋于 0 的位置)

图 3(a)对比了 2013 年 1 月 25 日和 2013 年 1 月 28 日的大气边界层高度日变化，图中各点代表激光雷达探测大气边界层的小时平均高度。可看出，25 日轻度灰霾天的边界层高度白天最高达 1100 m，夜间大致在 700—1000 m；28 日严重灰霾天全天边界层无明显变化，持续在 300—500 m。图 3(b)(c)，分别给出了 2013 年 1 月 25 日和 28 日 8:00 am 的水汽混合比和位温对比图，可以看出 28 日水汽含量明显高过 25 日，而 25 日水汽混合比随高度的变化反映了大气边界层高度位置；28 日位温随高度变化有一个明显的逆温层，这说明重霾天边界层偏稳定。由此看出，随着灰霾程度的加剧，昼夜大气边界层高

度变化明显减弱,在严重灰霾天气时,大气边界层高度昼夜变化不明显,且大气边界层高度日平均比轻度灰霾天下降约 500 m。

取 2013 年 1 月 25 日—28 日灰霾增加过程分析。图 3 给出 2013 年 1 月 25 日—28 日大气边界层与 $PM_{2.5}$、平均风速之间的关系,分别对大气边界层高度、$PM_{2.5}$ 和平均风速取日平均。由图 4(a)可以看出,灰霾急剧增加期边界层逐日降低,地面 $PM_{2.5}$ 浓度逐日升高。而导致这一现象的主要原因是在此次灰霾过程中,风速日平均值保持在 1.35—1.61 m/s (图 4(b)),持续的无风或微风导致大气湍流减弱,大气边界层高度降低且持续稳定,地面污染物浓度快速增加,形成严重污染。

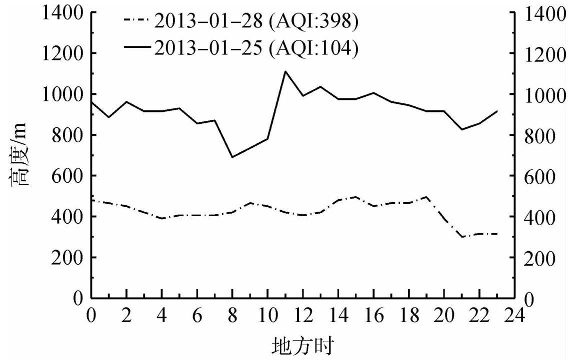

(a) 激光雷达探测的大气边界层高度

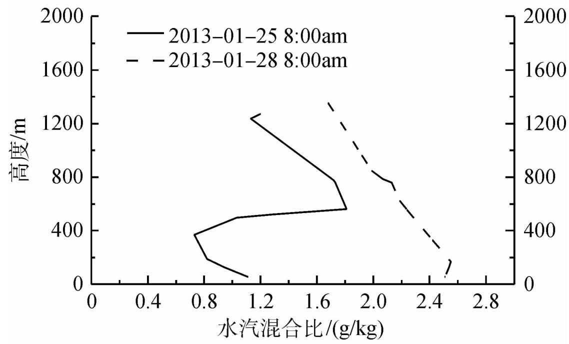

(b) 灰霾过程探空数据水汽混合比

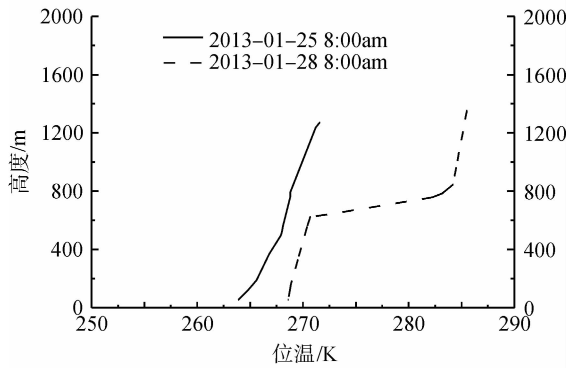

(c) 灰霾过程探空数据位温

图 3 2013 年 1 月 25 日至 28 日的大气边界高度、探空数据、水汽混合比及探空数据位温

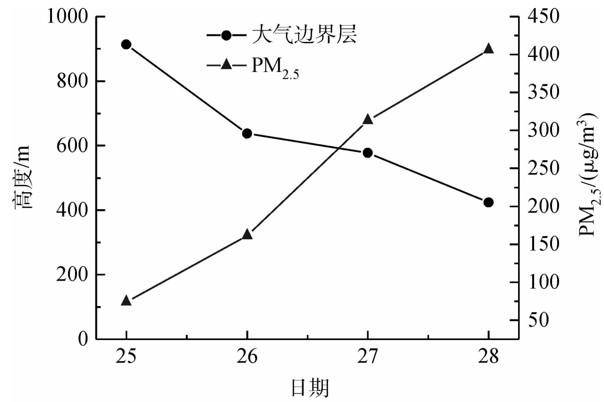

(a) 激光雷达探测日平均大气边界层高度与日平均$PM_{2.5}$

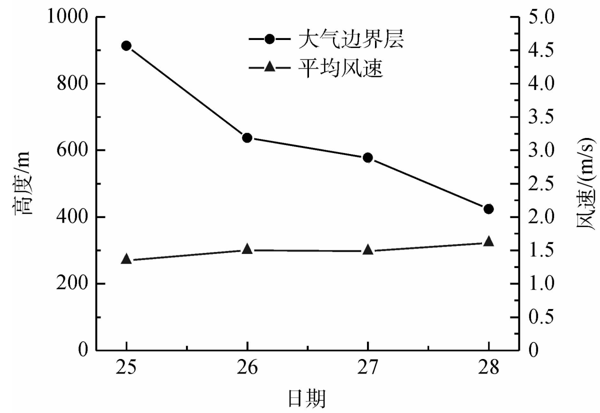

(b) 激光雷达探测日平均大气边界层高度与日平均风速

图 4 2013 年 1 月 25 日至 28 日灰霾过程激光雷达探测日平均大气边界层高与 $PM_{2.5}$、风速的关系

4 对比分析

为了分析激光雷达在灰霾期间大气边界层探测的结果,我们利用气象上探空综合评定法对北京气象站点探空资料数据进行处理,获得 2013 年 1 月每天北京时间 8:00 am 和 20:00 pm 的大气边界层高度,刘北平(1990)将该方法与干绝热曲线法对比相对误差为 2.7%—15%。本文将该方法获取的大气边界层高度与激光雷达有观测的灰霾天(AQI > 100)数据进行比较分析。图 5 是激光雷达和探空资料得到的大气边界层高度直方图,可以看出激光雷达探测的大气边界层高度月平均为 575 m,标准偏差为 155 m;探空资料探测的大气边界层高度月平均为 590 m,标准偏差为 178 m,对比结果显示利用激光雷达得到的大气边界层高度与探空数据结果有较好的一致性。同时,激光雷达与探空资料探测大气边界层高度的月平均差异为 86 m,考虑到两个观测站点之间的距离,该差异在两种测量方法可接受的精度范围之内。

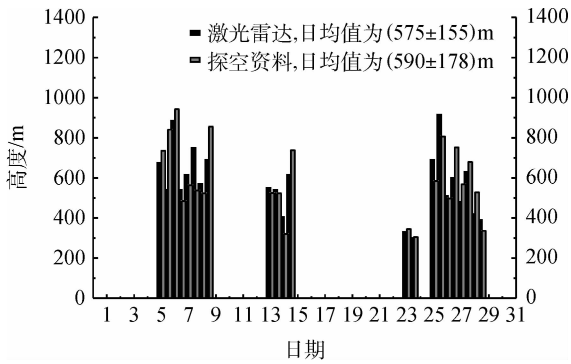

图 5 激光雷达与探空资料探测的 2013 年 1 月大气边界层高度直方图

激光雷达以其连续实时获取大气边界层高度的优势,可用于灰霾天气的边界层实时监测,并且梯度法在灰霾天气时的应用效果较好。但利用激光雷达梯度法探测大气边界层也有不足之处,表现在两方面:一是当天气晴朗时,大气中气溶胶消光不明显,较难找到 RCS 导数廓线信号明显变化位置;二是当存在大量低云时,激光雷达信号导数极值点有多处,还需人工辅助确定云高,区分云层与气溶胶层。

5 结 论

利用梯度法对激光雷达距离校正回波信号进行处理,得到了 2013 年 1 月北京地区的大气边界层高度,分析了在灰霾污染过程中,大气边界层高度与其他相关参数信息,如 $PM_{2.5}$、平均风速的相关性,得出以下结论:

(1)在大气边界层的探测能力方面,传统的气象探测手段由于受探测频次限制(如探空资料每天只有 8:00 am 和 20:00 pm 各一次探测),难以获得连续的大气边界层高度变化。而激光雷达梯度法是一种有效的探测灰霾天气的大气边界层高度的方法,可以很好地识别灰霾期间大气边界层实时变化状况,获得连续的大气边界层高度。

(2)灰霾期间,大气边界层高度有明显下降趋势。在严重灰霾天,平均大气边界层高度为 300—500 m 左右,且与轻度灰霾天相比,严重灰霾天气时大气边界层高度持续较低(例如一昼夜),加剧了大气污染物的积聚。

(3) 2013 年 1 月 25 日至 28 日灰霾污染过程中,通过对比激光雷达获得的大气边界层高度与近地面颗粒物 $PM_{2.5}$ 浓度,发现大气边界层高度与 PM2.5 呈明显负相关,大气边界层越低,$PM_{2.5}$ 越高。

获取大气边界层高度对于遥感监测近地面颗粒物质量浓度具有重要意义。本文对比激光雷达和探空探测的灰霾天大气边界层高度,结果具有较好的一致性,可为研究大气气溶胶垂直分布提供参考。

志 谢 感谢中国气象局公共气象服务中心提供气象资料帮助。

参考文献(References)

Fernald F G, Herman B M and Reagan J A. 1972. Determination of aerosol height distributions by lidar. Journal of Applied Meteorology, 11(3): 482 – 489 [DOI: 10.1175/1520 – 0450(1972)011 <0482:DOAHDB>2.0.CO;2]

Griffiths A D, Parkes S D, Chambers S D, Mccabe M F and Williams A G. 2013. Improved mixing height monitoring through a combination of lidar and radon measurements. Atmospheric Measurement Techniques, 6(2):207–218 [DOI: 10.5194/amt-6-207-2013]

韩道文, 刘文清, 张玉钧, 刘建国, 陆亦怀, 赵南京, 杨辉, 虞统. 2007. 激光雷达监测北京城区冬季边界层气溶胶. 大气与环境光学学报, 2(2):104–109

贺千山, 毛节泰. 2004. 微脉冲激光雷达及其应用研究进展. 气象科技, 32(4):219–224

Hennemuth B and Lammert A. 2006. Determination of the atmospheric boundary layer height from Radiosonde and Lidar backscatter. Boundary-Layer Meteorology, 120(1):181 – 200 [DOI: 10.1007/s10546-005-9035-3]

胡非, 洪钟祥, 雷孝恩. 2003. 大气边界层和大气环境研究进展. 大气科学, 27(4):712–728

Huang K, Zhuang G, Lin Y, Fu J S, Wang Q, Liu T, Zhang R, Jiang Y, Deng C, Fu Q, Hsu N C and Cao B. 2012. Typical types and formation mechanisms of haze in an Eastern Asia megacity, Shanghai. Atmospheric Chemistry and Physics, 12(1):105–124 [DOI:10.5194/acp-12-105-2012]

Klett J D. 1981. Stable analytical inversion solution for processing lidar returns. Applied Optics, 20(2):211 – 220 [DOI: 10.1364/AO.20.000211]

Lammert A and Bösenberg J. 2005. Determination of the convective boundary-layer height with laser remote sensing. Boundary-Layer Meteorology, 119(1):159–170 [DOI: 10.1007/s10546-005-9020-x]

廖国莲. 2005. 大气混合层厚度的计算方法及影响因子. 中山大学研究生学刊(自然科学、医学版), 26(4):66–73

刘诚, 明海, 王沛, 谢建平, 杨辉, 赵南京, 谢品华, 竹内延夫, 小池俊雄. 2006. 西藏那曲与北京郊区对流层气溶胶的微脉冲激光雷达测量. 光子学报, 35(9):1435–1439

刘北平. 1990. 确定大气混合层高度方法的研究. 环境科学研究, 3(1):8–12

毛敏娟, 蒋维楣, 吴晓庆, 戚福弟, 袁仁民, 方海涛, 刘东, 周军. 2006. 气象激光雷达的城市边界层探测. 环境科学学报, 26(10):1723

-1728
毛敏娟, 张寅超, 方海涛, 戚福弟, 邵石生, 胡欢陵, 周军. 2007. 机载激光雷达对青岛及周边海域的气溶胶探测. 地球物理学报, 50(2):370-376
潘鹄, 耿福海, 陈勇航, 贺千山, 张华, 亢燕铭, 毛晓琴, 王洪强. 2010. 利用微脉冲激光雷达分析上海地区一次灰霆过程. 环境科学学报, 30(11):2164-2173
邱金桓, 郑斯平, 黄其荣, 夏其林, 杨理权, 王文明, 潘继东, 孙金辉. 2003. 北京地区对流层中上部云和气溶胶的激光雷达探测. 大气科学, 27(1):1-7
Tsaknakis G, Papayannis A, Kokkalis P, Amiridis V, Kambezidis H D, Mamouri R E, Georgoussis G and Avdikos G. 2011. Inter-comparison of lidar and ceilometer retrievals for aerosol and planetary boundary layer profiling over Athens, Greece. Atmospheric Measurement Techniques, 4(6):1261-1273 [DOI: 10.5194/amt-4-1261-2011]
Wang Z, Cao X, Zhang L, Notholt J, Zhou B, Liu R and Zhang B. 2012. Lidar measurement of planetary boundary layer height and comparison with microwave profiling radiometer observation. Atmospheric Measurement Techniques, 5(8):1965-1972 [DOI: 10.5194/amt-5-1965-2012]
王珍珠, 李炬, 钟志庆, 刘东, 周军. 2008. 激光雷达探测北京城区夏季大气边界层. 应用光学, 29(1):96-100
吴兑. 2006. 再论都市霾与雾的区别. 气象, 32(4):9-15
吴兑, 邓雪娇, 毕雪岩, 李菲, 谭浩波. 2007. 都市霾与雾的区分及粤港澳的灰霾天气观测预报预警标准. 广东气象, 29(2):5-10, 28
Wu M, Wu D, Fan Q, Wang B M, Li H W and Fan S J. 2013. Study on the atmospheric boundary layer and its influence on regional air quality over the Pearl River delta. Atmospheric Chemistry and Physics Discussions, 13(3):6035-6066 [DOI:10.5194/acpd-13-6035-2013]
杨辉, 刘文清, 陆亦怀, 谢品华, 徐亮, 赵雪华, 虞统, 于建华. 2005. 北京城区大气边界层的激光雷达观测. 光学技术, 31(2):221-226
张改霞, 张寅超, 胡顺星, 刘小勤, 邵石生, 谭锟, 周军, 胡欢陵. 2004. AML-1 车载测污激光雷达探测大气边界层气溶胶. 强激光与粒子束, 16(3):286-290
张莹, 李正强. 2013. 利用细模态气溶胶光学厚度估计 $PM_{2.5}$. 遥感学报, 17(4):929-943 [DOI:10.11834/jrs.20133063]

遥感学报

启功先生创刊题名

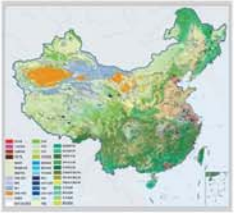

封面说明

About the Cover

2010年中国土地覆被遥感监测数据集（ChinaCover2010）

The China National Land Cover Data for 2010 (ChinaCover2010)

2010 年中国土地覆被遥感监测数据集（ChinaCover2010）由中国科学院遥感与数字地球研究所联合其他 9 个单位历时两年完成，应用 30 m 空间分辨率的环境星（HJ-1A/1B）数据，利用联合国粮农组织（FAO）的 LCCS 分类工具，构建了适用于中国生态特征的 38 类土地覆被分类系统，采用基于超算平台的数据预处理、面向对象的自动分类、地面调查获得的 10 万个野外样本以及雷达数据辅助分类相结合的方法，数据精度达到 85%。ChinaCover2010 主要基于国产卫星影像，将遥感与生态紧密结合，充足的野外样点以及严格的产品质量控制在最大程度上保证了数据的精度，可为中国生态环境变化评估以及生态系统碳估算提供基础数据支撑。（网址：http://www.chinacover.org.cn）

The China National Land Cover Data for 2010 (ChinaCover2010) has been completed after two years of team effort by the Institute of Remote Sensing and Digital Earth (RADI), Chinese Academy of Sciences (CAS), together with nine other institutions' participation. The HJ-1A/1B satellite at 30 m resolution is main data source. Based on the landscape features in China, 38 land cover classes have been defined using UN FAO Land Cover Classification System (LCCS). Super computers were used in the data preprocessing. An object-oriented method and a thorough field survey (about 100000 field samples) were used in the land cover classification, with radar imagery as auxiliary data. The overall accuracy of ChinaCover2010 is around 85%. Mainly based on domestic imagery, the products take advantage of various in situ data and strict quality control. ChinaCover2010 is a good dataset for ecological environment change assessment and terrestrial carbon budget studies. (Website: http://www.chinacover.org.cn)

遥感学报

JOURNAL OF REMOTE SENSING

YAOGAN XUEBAO（双月刊　1997年创刊）

第17卷　第4期　2013年7月25日

(Bimonthly, Started in 1997)

Vol.17 No.4 July 25, 2013

主　管	中国科学院	Superintended	by	Chinese Academy of Sciences
主　办	中国科学院遥感与数字地球研究所 中国地理学会环境遥感分会	Sponsored	by	Institute of Remote Sensing and Digital Earth,CAS The Associate on Environment Remote Sensing of China
主　编	顾行发	Editor-in-Chief		GU Xing-fa
编　辑	《遥感学报》编委会 北京市安外大屯路中国科学院遥感与数字地球研究所 邮编：100101　电话：86-10-64806643 http://www.jors.cn E-mail:jrs@irsa.ac.cn	Edited	by	Editorial Board of Journal of Remote Sensing Add: P.O.Box 9718, Beijing 100101, China Tel: 86-10-64806643 http://www.jors.cn E-mail: jrs@irsa.ac.cn
出　版	科学出版社	Published	by	Science Press
印刷装订	北京科信印刷有限公司	Printed	by	Beijing Kexin Printing Co. Ltd.
总发行	科学出版社 北京东黄城根北街16号 邮政编码：100717 电话：86-10-64017032 E-mail:sales_journal@mail.sciencep.com	Distributed	by	Science Press Add: 16 Donghuangchenggen North Street, Beijing 100717, China Tel: 86-10-64017032 E-mail: sales_journal@mail.sciencep.com
国外发行	中国国际图书贸易总公司 北京 399 信箱　邮政编码：100044	Overseas distributed	by	China International Book Trading Corporation Add: P.O.Box 399, Beijing 100044, China

中国标准连续出版物号：ISSN 1007-4619 / CN 11-3841/TP

CODEN YXAUAB

国内邮发代号：82-324

国外发行代号：BM 1002

定价：70.00元

ISSN 1007-4619

07>

9 771007 461132

国内外公开发行